Volume 1 | Number 1 | Jan 2013 | Pages 1–100

Nanoscale

www.rsc.org/nanoscale

ROYAL SOCIETY OF CHEMISTRY

ROYAL SOCIETY OF CHEMISTRY

www.rsc.org/nanoscale

Nanoscale

ARTICLE

High quality reduced graphene oxide flakes by fast kinetically controlled and clean indirect UV-induced radical reduction

Roman Flyunt,*[a] Wolfgang Knolle,[a] Axel Kahnt,[b] Christian E. Halbig,[c] Andriy Lotnyk,[a] Tilmann Häupl,[a] Andrea Prager,[a] Siegfried Eigler,[c,d] and Bernd Abel*[a]

This work highlights a surprisingly simple and kinetically controlled highly efficient indirect method for the production of high quality reduced graphene oxide (rGO) flaces via UV irradiation of aqueous dispersions of graphene oxide (GO), in which the GO is not excited directly. While the direct photoexcitation of aqueous GO (when GO is the only light-absorbing component) takes several hours of reaction time at ambient temperature (4 h) leading only to a partial GO reduction, the addition of small amounts of isopropanol and acetone (2 and 1 %) leads to a dramatically shortened reaction time by more than two orders of magnitude (2 min) and a very efficient and soft reduction of graphene oxide. This method avoids the formation of non-volatile species and in turn contamination of the produced rGO and it is based on the highly efficient generation of reducing carbon centered isopropanol radicals via the reaction of triplet acetone with isopropanol. While the direct photolysis of GO dispersions easily leads to degradation of the carbon lattice of GO and thus to a relatively low electric conductivity of the films of flakes, our indirect photoreduction of GO instead largely avoids the formation of defects, keeping the carbon lattice intact. Mechanisms of the direct and indirect photoreduction of GO have been elucidated and compared. Raman spectroscopy, XPS and conductivity measurements prove the efficiency of the indirect photoreduction in comparison to the state-of-the-art reduction method for GO (hydriodic acid / trifluoroacetic acid). The rapid reduction times and water solvent containing only a small amounts of isopropanol and acetone may allow easy process up-scaling for technical applications and low-energy consumption.

Introduction

A decade after the outstanding experiments with graphene in 2004 [1] enormous research activities in many fields of science emerged. The reasons for this are the unique properties of graphene such as very high electrical and thermal conductivity, ultra-high carrier mobility, optical transparency, high mechanical, chemical and physical stability and many more. The most promising applications of graphene are nano-electronic devices, [1-5] supercapacitors, [6] solar cells, [7, 8] gas sensors,[9] energy-storage materials,[10, 11] in bioapplications[7, 8, 12-14] or as a new membrane material.[15]

High purity graphene obtained by mechanical exfoliation of graphite, chemical vapor deposition growth from carbon precursors or epitaxial growth on silicon carbide could not be used for large-scale applications due to its high costs. The most effective alternative to obtain large quantities of single layered graphene-like materials is through the reduction of GO. The desoxygenation of GO can be accomplished thermally, chemically, radiation-chemically or photochemically as reviewed recently.[16, 17] A thermal approach has a major disadvantage of a high energy waste and the degeneration of the carbon grid as a consequence of CO and CO_2 formation.[18]

The most important drawbacks of chemical reduction methods are use of hazardous chemicals like hydrazine or derivatives, long treatment times of several hours, high temperatures, formation of environmentally dangerous products from the reductant and contamination of reduced GO by non-volatile oxidation products of the reducing agent. In particular, the latter contaminations are a technological problem for separating rGO. In this sense, a significant improvement in the GO reduction strategy has been demonstrated in the studies describing the efficiencies of $LiAlH_4$, [19] substituted borohydrides[20] and thiourea dioxide (a common industrial reductant)[21] as reducing agents.

Photoreduction of GO has been explored as an alternative strategy to chemical reduction of GO and was recently reviewed, both in solution and in films.[22] Since we study the phototransformations of GO in aqueous dispersions, we will shortly describe the progress of the latter. Photoreduction of GO aqueous dispersions in the absence of photocatalysts, reducing agents and dispersants by intense UV irradiation (1 W/cm^2, 50 W short arc Hg bulb) has been studied.[23] After 15 h of irradiation, GO was partially reduced as evidenced from the change of C/O ratio between 2.3 and 4.5. Irradiation of GO aqueous dispersions containing 20% methanol as sacrificial

a. Leibniz-Institut für Oberflächenmodifizierung (IOM), Permoserstr. 15, D-04303 Leipzig, Germany; Email: roman.flyunt@iom-leipzig.de
b. Department of Chemistry and Pharmacy & Interdisciplinary Center for Molecular Materials (ICMM), Friedrich-Alexander-Universität Erlangen-Nürnberg (FAU), 91058 Erlangen, Germany
c. Department of Chemistry and Pharmacy & Central Institute for New Materials and Processing Technology, Friedrich-Alexander-Universität Erlangen-Nürnberg (FAU), 90762 Fürth, Germany.
d) Department of Chemistry and Chemical Engineering, Chalmers University of Technology, 41258 Göteborg, Sweden.
*) bernd.abel@iom-leipzig.de; Roman.Flyunt@iom-leipzig.de
Electronic Supplementary Information (ESI) available: [Experimental details, calculations on energy consumption, reaction schemes, analysis (optical density changes, Raman and XPS). See DOI: 10.1039/x0xx00000

Nanoscale Accepted Manuscript

reagent with UV or visible light leads to hydrogen generation, which was assigned to a water splitting reaction, photocatalyzed by GO as semiconductor.[24] Six hours of irradiation under mercury lamp led to a partly photoreduced GO with only a hundred times reduced resistivity. In another study films of highly conductive rGO with a conductivity of 4680 S x m^{-1} was obtained, the highest reported value for photochemically reduced films of GO.[25] However, a natural reduced nicotinamine adeninedinucleotide NAD(P)H model, Hantzsch 1,4-dihydropyridine (HEH) under 500 W high–pressure mercury lamp was necessary and ethyl acetate extraction of HEH and its aromatic pyridine product was mandatory to achieve highly conductive films. Among the series of the works Jang *et al.* reported the photocatalytic synthesis of water-dispersible rGO, with a high conductivity value of 1727 S x m^{-1} after 6 h of irradiation of GO/TiO$_2$ solutions by means of 500 W Hg arc lamp.

Recently, we have reported a basic study on the radiation-induced reduction of GO, using water as solvent, where only a small content (at most 2 wt.-%) of 2-PrOH are required to generate highly reducing free radicals capable to efficiently reduce GO.[26] Among all reducing species studied the 1-hydroxy-1methylethyl radicals (CH$_3$)$_2$C$^{\bullet}$(OH) derived from the reaction of 2-PrOH with radiolytically generated $^{\bullet}$OH radicals (see reaction 4 further below) seem to be the most promising one. This is because they are a strong reductant with a redox potential of -1.8 V *vs.* NHE [27] and their precursor and final product from them, 2-PrOH and acetone, respectively, are not compounds of a major environmental or technological concern. The (CH$_3$)$_2$C$\bullet$(OH) radicals can also be easily produced photochemically by UV–irradiation of the 2-PrOH/acetone system with a quantum yield of approximately unity (quantitative reaction).[28]

Here, we demonstrate the highly efficient indirect UV-induced reduction of GO by (CH$_3$)$_2$C$\bullet$(OH) radicals generated from acetone/2-PrOH (see Scheme in Fig. 1). The reaction conditions accelerate the photoinduced reduction more than 100 times (Figure 1) and the method nearly completely avoids the formation of lattice defects. Furthermore, the method is of environmental compatibility, of low cost, scalable,[29] and overcomes the drawbacks described in any of the aforementioned approaches, such as avoiding contaminations.

Results and Discussion

Mechanistic study of the photoinduced reduction of GO

The quality of GO depends strongly on the preparation conditions,[30] as not only the contribution of functional groups but also the integrity of the carbon framework differs from one synthetic method to another. A variation in the density of defects up to several % is well known.[30, 31] In this work, we use two types of GO. One commercial source of GO from Cheap Tubes (CT-GO) and oxo-functionalized graphene (oxo-G$_1$), which exhibits an average density of defects of only 0.3% within the carbon skeleton (Figure 3a).[30] In contrast CT-GO bears defects of several percent. Since the average density of

defects in oxo-G$_1$ is quite low, this material enables chemical functionalization of the basal plain, while functionalization at defect sites plays only minor role. Moreover, the functional groups in oxo-G$_1$ have been analyzed previously.[32-35] They mostly are hydroxyl, epoxy and organosulfate groups, located on both sides of the basal plain.[35-39] Recently, we proved that the carbon framework in oxo-G$_1$ is thermally stable up to 100 °C, and that the functionalization of oxo-G$_1$ is possible without harming the carbon framework.[33, 40, 41] Oxo-G$_1$ is prepared from natural graphite by the controlled oxidation in sulfuric acid using potassium permanganate and sodium nitrate as oxidants at a temperature of 5-10 °C, followed by aqueous work-up at the same temperature.[34] This procedure largely prevents the formation of defects and the defect density can be estimated to 0.3%. Hydrogen peroxide is subsequently used to make manganese salts soluble. The multilayered oxo-functionalized material is purified by repeated centrifugation and redispersion in cold water, until the pH of the supernatant is about 6. Delaminated in water yielded oxo-G$_1$ flakes.[34]
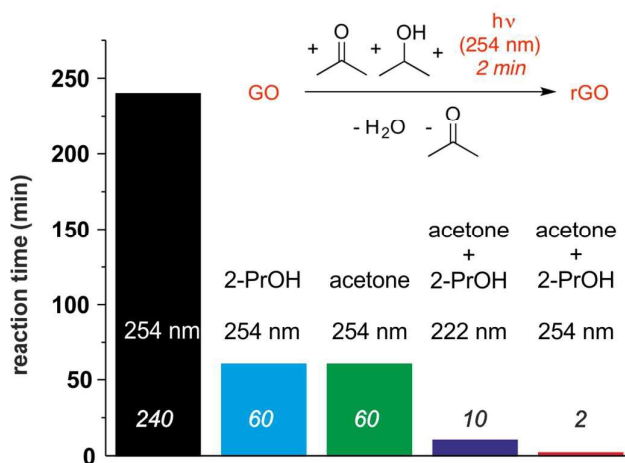
Figure 1. Illustration of the reaction times observed for the photochemical reduction of GO. GO in water: no additive (black, 240 min, 254 nm); 2% 2-PrOH (blue), 60 min, 254 nm); 1% acetone (green, 60 min, 254 nm); 1% acetone and 2% 2-PrOH (violet, 10 min, 222 nm); 1% acetone and 2% 2-PrOH (red, 2 min, 254 nm).

For the mechanistic study we used CT-GO, because reduced CT-GO remains more stably dispersed, assumedly due to functional groups at edges of flakes and especially defect sites. The direct photochemical treatment CT-GO in water, where the light is solely absorbed by GO, only a low reduction degree and long reaction times of about 4 h are measured (Scheme 1, 1-3, Table 1). The reduction efficiency can be improved when efficient hole/•OH radical scavengers like 2-PrOH are added.[42] Highly reducing α-hydroxyalkyl radicals are formed due to the reaction with light generated holes (5). Scavenging the holes increases the lifetime of e$_{CB}$− enhancing the reduction efficiency for GO (2). The undesired GO oxidation by holes and/or hydroxyl radicals (4) is also suppressed. In the system with 2 wt.-% 2-PrOH (the absorbance of the latter is negligible), the process is indeed 4 times faster compared to the system with pure GO (Table 1). Even more interesting is the fact that an absorption maximum of the treated dispersion

shifts from 226 nm to 260 nm, which is mostly due to formation of rGO with a small extent arising from the absorption of formed acetone. This observation evidences that the reduction process of GO proceeds *via* the mechanism depicted by the sequence of the reactions 1-4 and in part by 2-PrOH reduction, as illustrated in Scheme 2 (9-10).

Table 1. Results of UV-irradiation of CT-GO in 0.04 g l^{-1} aqueous nitrogen-saturated dispersions at pH 5 containing different additives under the illumination with 254 nm photons.

System	Reaction time, h	Remarks
Pure GO	3.5-4 h	λ^0_{max} = 227 nm, final λ_{max} = 240 nm
GO + 2 % 2-PrOH	1 h	λ^0_{max} = 226 nm, final λ_{max} = 260 nm
GO + 1 % Acetone	1 h	λ^0_{max} = 263 nm*, final λ_{max} = 269 nm, strong sedimentation after 75 min
GO + 1 % Acetone + 2 % 2-PrOH	2 min	λ^0_{max} = 263 nm*, final λ_{max} = 266 nm, no sedimentation

* absorption maximum of the dispersion at 263 nm because of the acetone content.

Next, we found that the addition of 1 wt.-% of acetone also accelerates the phototransformation of GO – the reaction time has been shortened to 1 h (Table 1). This 4-fold acceleration effect is most likely due to the scavenging of e$_{CB}$– by acetone (6). Here, an acetone radical anion is formed which should promptly be protonated giving a strongly reducing alkyl radical $(CH_3)_2C\bullet(OH)$, the same as generated via reaction 4 with 86 % yield.[43] The fate of the holes generated in this system is unclear, but at least recombination of holes and electrons is suppressed. One can propose that the holes could be transformed first to hydroxyl radicals (3), which further react with acetone *via* H-abstraction (see eq. S1, Supporting Information) with a rate constant of $k = 1.3 \times 10^8$ dm^3 mol^{-1} s^{-1}).[44] It can also be expected that hydroxyl radicals can induce further lattice defects in GO.

$$GO + h\nu \longrightarrow GO^* \longrightarrow h_{vb}^+ + e_{cb}^- \quad (1)$$

$$e_{cb}^- + GO \longrightarrow GO^{\bullet-} \Longrightarrow rGO \quad (2)$$

$$h_{vb}^+ + H_2O \longrightarrow \bullet OH + H^+ \quad (3)$$

$$\bullet OH + \underset{OH}{\bigvee} \longrightarrow H_2O + \underset{OH}{\bigvee} \quad (4)$$

$$h_{vb}^+ + \underset{OH}{\bigvee} \longrightarrow \underset{OH}{\bigvee} + H^+ \quad (5)$$

$$e_{cb}^- + \underset{O}{\bigvee} + H^+ \longrightarrow \underset{OH}{\bigvee} \quad (6)$$
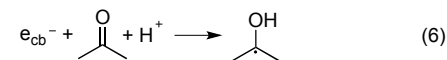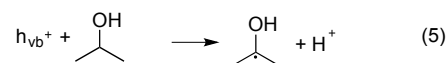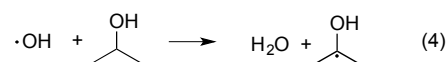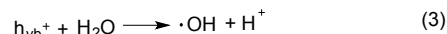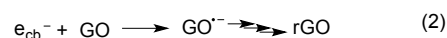
Scheme 1. Reaction scheme illustrating the ideal direct photochemical reduction of GO (1-3) and accompanied radical reactions with additives, such as 2-PrOH and acetone, respectively (4-6). Addition of either 2-PrOH or acetone reduces the reaction time of GO from about 4 h to 1 h.

The redox potential of the formed alkyl radicals is not known (S1). However, some reactions have been reported in the literature, which confirm weak oxidative properties.[45] In contrast to the system of GO alone or with 2-PrOH, the strong absorption of acetone around 260 nm renders difficult the shift of an absorption maximum related to photo transformed GO in this system. Another difference is that the light in the latter system is absorbed by both, GO and acetone. One of the major species generated in this system is triplet acetone. The latter is known as an efficient H-abstractor from weak C-H bonds.[28] The great majority of hydrogen atoms in GO is present in the form of hydroxyl and carboxyl groups, i.e. they are hardly abstractable[44] and the contribution of this route can be neglected. Some examples of addition of triplet acetone to unsaturated C=C bonds are known as well.[28] If this takes place in our system, it will not lead to rGO as the end product. Two other alternatives for triplet acetone would be one-electron oxidation of GO or energy transfer to GO, generating radical-cation GO$^{\bullet+}$ or excited GO* species, respectively. However, both of them will not end-up as rGO. Another reaction pathway could be the homolytic cleavage of triplet acetone leading to the generation of methyl and 1-oxoethyl radicals (S2).[46] This reaction is well-described for the gaseous phase. The CH$_3\bullet$ radical is redox-inert and the CH$_3$C$\bullet$=O is a radical of moderate reducing properties,[47] however, the related hydrate species, CH$_3$C$\bullet$(OH)$_2$, was reported as a stronger reducing radical, which may further reduce GO (S3).[48] Summarizing, one can state that the photochemical system consisting of oxygen-free aqueous GO and acetone could lead to only partial reduction of GO. For this reasons, no further investigations of this system were undertaken.

Indirect photoreduction of GO with acetone/2-PrOH

In contrast to the above studies the photoreduction of GO in water with of acetone/2-PrOH(1% and 2%, respectively) accelerates and a reduced reduction time of only 2 min was observed, in contrast to 4 h (Figure 1). The mechanism behind that accelerated reaction must be very different from the ones described before for solely added 2-PrOH and acetone, respectively, and it can be assumed that those reaction mechanism contribute less than 7%, based on the data presented in Table 1 (calculated as 100% x 2 min/60 min multiplied by a factor of 2). Thus, the photochemistry of the acetone/2-PrOH couple must be considered [28] and it can be described by the reactions 7 and 8 *via* triplet acetone formation and reaction to 2-PrOH radicals.

The lifetime of triplet acetone in aqueous 0.05 M acetone solution without any quencher is 50 ± 2 µs (7).[28] This value is shortening in the presence of the triplet acetone quenchers. The triplet acetone reacts with 2-PrOH *via* H-atom abstraction with a rate constant of 9.7×10^5 dm^3 mol^{-1} s^{-1} (8). Thus, at 2-wt.% of 2-PrOH (corresponding to 0.25 M of 2-PrOH) a lifetime of 12 µs is calculated. As a result of the reactions 7 and 8, two carbon centered isopropanol radicals of $(CH_3)_2C\bullet(OH)$ are generated.

To further prove this mechanism, we conducted the process at 222 nm and 254 nm, respectively, because the reduction should be

ARTICLE   Nanoscale

more efficient for the latter one. For this, we employed two different light sources, which generate the 222 nm and 254 nm photons, i.e. close to absorption maxima of GO (226 nm for CT-GO and 235 nm for oxo-G_1) and acetone (265 nm), respectively.

Absorption of acetone at 222 nm corresponds to ca. 10% of the value at 254 nm. In contrast, the absorbance of GO at the wavelengths of our interest (222 and 254 nm) differs to a much smaller extend. The corresponding ratios of A_{222}/A_{254} are equal to 1.00/0.96 for oxo-G_1 and 1.00/0.87 for CT-GO, respectively.

A typical diagram for the optical changes (222 nm) in a nitrogen-saturated aqueous dispersion, consisting oxo-G_1, 0.35 wt.-% acetone, 2 wt.-% 2-PrOH, is shown in Figure 2. The absorption at $\lambda > 250$ nm is continuously evolving with photoirradiation time (Figure S1). Here, it should be pointed out that the absorbance of acetone is negligible at $\lambda > 350$ nm. Therefore, the formation of reduced oxo-G_1 can be monitored at any wavelengths > 350 nm, as shown in the inset to Figure 2. The maximum absorbance is reached within 10 min. After reaching the optical maximum a slight decrease of absorbance has been observed. The latter is most likely due to agglomeration of reduced oxo-G_1. The absorption maximum at 258 nm for starting dispersion has been shifted to 264 nm after 10 minutes irradiation (a corresponding maximum of 266 nm has been determined for the same system irradiated at 254 nm).
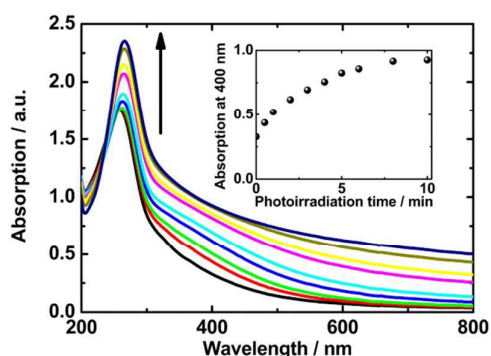
Figure 2. Change of the optical absorption for a nitrogen saturated aqueous dispersion of oxo-G_1 (0.05 g/l oxo-G_1, 0.35 wt.-% of acetone and 2 wt.-% of 2-PrOH at natural pH 5) under illumination at 222 nm from 0 to 10 min photoirradiation time. Inset change of the optical absorption at 400 nm upon photoirradiation time.

The photoreduction of oxo-G_1 initiated at 254 nm is apparently 5 times faster than at 222 nm (2 min). This is due to two factors, namely that the 254 nm light source has a 3 times higher irradiance than 222 nm lamp (see experimental methods) and the percentage of the 254 nm light absorbed by acetone is about eight times higher than at 222 nm (Table 2).

Table 2. Comparison of the indirect photoreduction of oxo-G_1 and CT-GO in aqueous dispersions (containing 2 wt.-% 2-PrOH and 0.35 wt.-% acetone at pH 5) induced at 222 nm and 254 nm, respectively.

[GO] and its type / wavelength / atmosphere	Reaction time, min	Absorbed energy, J	Total photons absorbed, Einstein	*Photons absorbed by acetone, %
0.05 g/l oxo-G_1 222 nm / N_2	10	11.6	2.16×10^{-5}	4.2
0.05 g/l oxo-G_1 254 nm / N_2	2	5.8	1.22×10^{-5}	31
0.033 g/l CT-GO 222 nm / N_2	9	10.4	1.94×10^{-5}	4.7
0.033 g/l CT-GO 254 nm / N_2	1.67	4.8	1.02×10^{-5}	39

* these values correspond to an initial stage of photoirradiation, they will be changed within the process, since formed rGO possesses a higher absorptivity than the starting GO.

The same principal picture was observed in the case of CT-GO containing system (Table 2). Here, the 254 nm light source was also more efficient – the determined reaction time was shorter than 2 min. Again, the process under 222 nm illumination is considerably longer (measured reaction time 9 min), which can be explained similarly to the oxo-G_1 system.

Thus, under the conditions studied in this work the use of 254 nm light source provides a more efficient way for GO photoreduction with shorter reaction times and a lower absorbed energy (Table 2). For the reaction of $(CH_3)_2C\bullet(OH)$ radicals with GO we assume an electron-transfer mechanism (the most typical pathway for these radicals in the reactions with electron-accepting partners, see [44], [45]) *via* generating GO radical "anions" (9) which further eliminate hydroxide anions or water molecules forming rGO by restoration of C=C bonds (10).
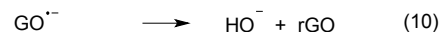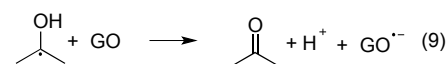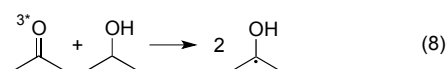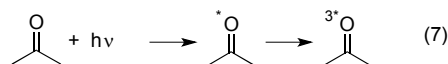
Scheme 2. Illustration of the indirect photochemical reduction of GO *via* acetone excitation and formation of triplet acetone (7), followed by the formation of two 2-PrOH radicals (8). Next, GO is reduced by the electron transfer from 2-PrOH radicals (9) and the process is accompanied by desoxygenation (10).

In total, acetone/2-PrOH at 254 nm irradiation is generating two $(CH_3)_2C\bullet(OH)$ radicals. Those radicals subsequently reduce GO forming rGO and water and acetone as side-products (11).
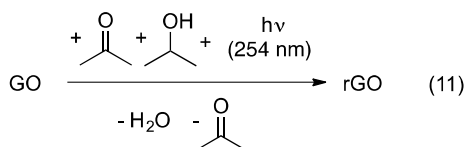
Scheme 3. Illustration of the total indirect reaction of GO with UV-light, mediated by acetone/2-PrOH forming rGO with water and acetone as side-products.

The relative reactivity of different GO samples can be roughly estimated in the following way. Since the reaction times for the photoreduction of different types of GO samples using the 254 nm photons were approximately equal (2 min for oxo-G_1 and 1.67 min for CT-GO) and the number of 254 nm photons absorbed by acetone in oxo-G_1 dispersion was smaller, oxo-G_1 should possess a higher reactivity, because the concentration of oxo-G_1 (0.05 g/l) was 50% higher compared to CT-GO (0.033 g/l). It might reflect the fact that oxo-G_1 possesses the lower density in terms of lattice defects in basal plain compared to CT-GO.[31, 49 41, 50 18, 33]

Reaction time is increasing proportionally to CT-GO concentration, for example, from 1.25 min to ca. 7 min upon the change of CT-GO concentration from 0.025 to 0.125 g/L under otherwise identical conditions. Variation of 2-PrOH concentrations from 1 to 5 wt.-% at constant CT-GO and acetone concentration did not change the reaction time, showing that 1 wt.-% of 2-PrOH is sufficient to scavenge all triplet acetone generated in the system.

Characterization of the products by Raman spectroscopy

Raman spectroscopy is recognized as a very sensitive tool for the characterization of carbon nanomaterials. But in fact, Raman spectra of rGO with lattice defects of several % are difficult to analyze, because of the very little spectral changes between GO and rGO. Recently, spectra of such defective rGO were critically and systematically evaluated.[51] According to that systematic analysis a high degree of reduction is indicated for reduced CT-GO (Figure S2 and Table S1).
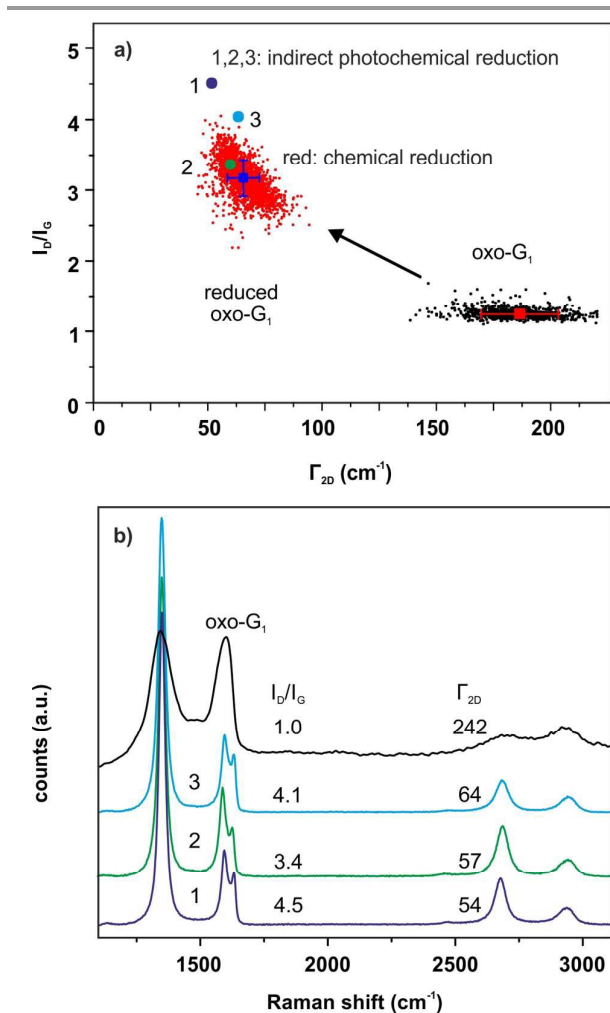
Figure 3. a) Statistical Raman spectroscopic analysis of hydriodic acid / trifluoroacetic acid reduced oxo-G_1 (red) and oxo-G_1 (black), respectively. The numbered spectra 1-3 reflect data extracted from Raman spectra of indirect photochemically reduced flakes of oxo-G_1. b) Individual Raman spectra of oxo-G_1 and indirect photochemically reduced flakes of oxo-G_1 with Γ_{2D} values between 54 cm^{-1} and 64 cm^{-1}.

However, the reduction of oxo-G_1 can be determined quantitatively.[52-54] Reduced flakes of oxo-G_1 were therefore deposited on SiO$_2$/Si substrates for Raman measurements and while the D, G and 2D bands of oxo-G_1 are broad, very sharp peaks with I_D/I_G ratios of up to 4 are found, indicating a very efficient reduction with a residual density of defects of roughly 0.3%. Statistical Raman spectroscopy conducted on oxo-G_1 flakes reveals an average full-width at half-maximum of the 2D band (Γ_{2D}) of about 180 cm^{-1} and after chemical reduction with vapor of hydriodic acid / trifuoroacetic acid Γ_{2D} values decreased to about 65 cm^{-1} (Figure 3). For the indirect photochemical reduction method described here, spectra of individual flakes were measured and Γ_{2D} values between 54 cm^{-1} and 64 cm^{-1} were found (Figures 3). Thus, it can be concluded that the quality of reduced oxo-G_1 is at least as high as the most potent chemical reduction method.[41, 55, 56]

Characterization of the products by XPS

XPS is a standard technique to determine the reduction degree of GO. High resolution C 1s spectra are shown in Figure 4 that reveal a high efficiency of the reduction method. The most narrow XPS C 1s peak is recorded for the indirectly photoreduced CT-GO, while CT-GO and hydrazine reduced CT-GO and electron beam reduced CT-GO possess broader peaks. According to the literature it is possible to quantitatively convolute the spectra according to six different carbon species.[57] The results of that approach are depicted in Figure S3 and Table S2.

Characterization of the products by conductivity of films

GO is supposed to be almost insulating, however a conductivity of 5×10^{-4} S x m^{-1} was reported in the literature.[25] Compared to this value the conductivity of reduced CT-GO and reduced oxo-G$_1$ increased by respectively 6 and 7 orders of magnitude (Table 3).

Table 3. Conductivity values and C/O ratios for reduced CT-GO and reduced oxo-G$_1$ films obtained by different treatments of GO aqueous dispersions.

	CT-GO		oxo-G$_1$	
	conductivity, S x m^{-1}	C/O *	conductivity, S x m^{-1}	C/O *
no treatment	5×10^{-4} **	2.3	5×10^{-4} **	2.3
hydrazine	400	6.9	4900	7.1
EB	480	7.4	5400	10.9
Indirect photoreduction	520	8.4	5500	8.4

* - the calculated C/O ratios represent a lower limit values. A certain amount of oxygen originates from of Si and S compounds which were detected in the range of a few percents. However, as their stoichiometry with oxygen is unknown, a correction for the C/O ratio is unreliable.

** - adopted from the literature.[25]

The conductivities of films are roughly 500 S x m^{-1} and 5000 S x m^{-1} for films of reduced CT-GO and reduced oxo-G$_1$, respectively. Those values are at least as high as the best values reported yet for photoreduced GO.[25] However, it must be taken into account that flake size, film morphology and potential trapping of solvent molecules may possess a huge influence on the bulk conductivity. Moreover, electron beam (EB) and indirect photoreduction methods are well comparable with hydrazine method. Also the C/O ratios for reduced CT-GO and reduced oxo-G$_1$ obtained by hydrazine or indirect photoreduction are similar (Table 3). The approximately 10 times better conductivity of reduced oxo-G$_1$ over reduced CT-GO is most likely due to a much lower defect density within the carbon framework.[34]

Conclusions

The fast and efficient indirect photoreduction of GO in the presence of acetone/2-PrOH was highlighted. The surprizing finding here is that the reduction reaction is more than 100 and 30 times faster, compared to the direct GO phototransformation of GO without additives or in the presence of either acetone or 2-PrOH alone, respectively. As we show here, this acceleration is due to highly efficient generation of the strongly reducing free radicals derived from the reaction of triplet acetone with 2-PrOH. Most importantly, it can be concluded that reactions paths that lead to defect formation are suppressed by this method, as evidenced by Raman spectrosocpy conducted on oxo-G$_1$. The method is at least as efficient (if not superior) as the best chemical reduction methods. A substantial advantage of the method is that only volatile side-products are formed that can be easily removed from rGO (acetone, 2-PrOH and water). No toxic or explosive reagents are needed and the necessary energy input is at least 5 times lower compared to laser-induced desoxygenation of GO (see SI for calculation on energy consumption), a method that can be expected to introduce lattice defects.[18, 58]

In view of our results, it can be expected that the method of indirect photoreduction of GO highlighted here may be a solid basis for the development of a large scale production of rGO, because of the high efficiency, environmental compatibility and low cost. Thus, the production of supercapacitors and other applications may benefit from the indirect photochemical reduction method.

Acknowledgements

References

1.   K. S. Novoselov, A. K. Geim, S. V. Morozov, D. Jiang, Y. Zhang, S. V. Dubonos, I. V. Grigorieva and A. A. Firsov, *Science*, 2004, 306, 666-669.
2.   A. K. Geim and K. S. Novoselov, *Nature Mater.*, 2007, 6, 183-191.
3.   D. C. Elias, R. R. Nair, T. M. G. Mohiuddin, S. V. Morozov, P. Blake, M. P. Halsall, A. C. Ferrari, D. W. Boukhvalov, M. I. Katsnelson, A. K. Geim and K. S. Novoselov, *Science*, 2009, 323, 610-613.
4.   M. J. Allen, V. C. Tung and R. B. Kaner, *Chem. Rev.*, 2010, 110, 132-145.
5.   L. Vicarelli, S. J. Heerema, C. Dekker and H. W. Zandbergen, *ACS Nano*, 2015, 9, 3428-3435.

6.   Y. Shao, M. F. El-Kady, L. J. Wang, Q. Zhang, Y. Li, H. Wang, M. F. Mousavi and R. B. Kaner, *Chem. Soc. Rev.*, 2015, 44, 3639-3665.

7.   F. Schedin, A. K. Geim, S. V. Morozov, E. W. Hill, P. Blake, M. I. Katsnelson and K. S. Novoselov, *Nature Mater.*, 2007, 6, 652-655.

8.   S. K. Balasingam and Y. Jun, *Isr. J. Chem.*, 2015, 55, 955-965.

9.   W. Yuan and G. Shi, *J. Mater. Chem. A*, 2013, 1, 10078.

10.   J. Zhu, D. Yang, Z. Yin, Q. Yan and H. Zhang, *Small*, 2014, 10, 3480-3498.

11.   Z. Wang, S. Eigler, Y. Ishii, Y. Hu, C. Papp, O. Lytken, H.-P. Steinrück and M. Halik, *J. Mater. Chem. C*, 2015, 3, 8595-8604.

12.   Y. Wang, Z. H. Li, J. Wang, J. H. Li and Y. H. Lin, *Trends Biotechnol.*, 2011, 29, 205-212.

13.   C. Chung, Y. K. Kim, D. Shin, S. R. Ryoo, B. H. Hong and D. H. Min, *Acc. Chem. Res.*, 2013, 46, 2211-2224.

14.   H. Pieper, S. Chercheja, S. Eigler, C. Halbig, M. Fillipović and A. Mokhir, *Angew. Chem. Int. Ed.*, 2016, 55, 405-407.

15.   R. K. Joshi, S. Alwarappan, M. Yoshimura, V. Sahajwalla and Y. Nishina, *Appl. Mat. Today*, 2015, 1, 1-12.

16.   C. K. Chua and M. Pumera, *Chem. Soc. Rev.*, 2014, 43, 291-312.

17.   R. Flyunt, W. Knolle, A. Kahnt, S. Eigler, A. Lotnyk, T. Häupl, A. Prager, D. Guldi and B. Abel, *Am. J. Nano Res. and Appl.*, 2014, 2, 9-18.

18.   S. Eigler, C. Dotzer and A. Hirsch, *Carbon*, 2012, 50, 3666-3673.

19.   A. Ambrosi, C. K. Chua, A. Bonanni and M. Pumera, *Chem. Mater.*, 2012, 24, 2292-2298.

20.   C. K. Chua and M. Pumera, *J Mater Chem A*, 2013, 1, 1892-1898.

21.   C. K. Chua, A. Ambrosi and M. Pumera, *J. Mater. Chem.*, 2012, 22, 11054-11061.

22.   Y.-L. Zhang, L. Guo, H. Xia, Q.-D. Chen, J. Feng and H.-B. Sun, *Advanced Optical Materials*, 2014, 2, 10-28.

23.   L. Guardia, S. Villar-Rodil, J. I. Paredes, R. Rozada, A. Martínez-Alonso and J. M. D. Tascón, *Carbon*, 2012, 50, 1014-1024.

24.   T. F. Yeh, J. M. Syu, C. Cheng, T. H. Chang and H. S. Teng, *Adv. Funct. Mater.*, 2010, 20, 2255-2262.

25.   H.-H. Zhang, Q. Liu, K. Feng, B. Chen, C.-H. Tung and L.-Z. Wu, *Langmuir*, 2012, 28, 8224-8229.

26.   R. Flyunt, W. Knolle, A. Kahnt, A. Prager, A. Lotnyk, J. Malig, D. Guldi and A. Abel, *Int. J. Radiat. Biol.*, 2014, 90, 486-494.

27.   P. Wardman, *J. Phys. Chem. Ref. Data*, 1989, 18, 1637-1755.

28.   G. Porter, S. K. Dogra, R. O. Loutfy, S. E. Sugamori and R. W. Yip, *J. Chem. Soc., Farad. Trans 1: Phys. Chem. in Cond Phases*, 1973, 69, 1462-1474.

29.   DE 10 2012 024 329.4, 2012.

30.   S. Eigler and A. Hirsch, *Angew. Chem. Int. Ed.*, 2014, 53, 7720-7738.

31.   S. Eigler, *Chem. Commun.*, 2015, 51, 3162-3165.

32.   S. Eigler, Y. Hu, Y. Ishii and A. Hirsch, *Nanoscale*, 2013, 5, 12136-12139.

33.   S. Eigler, S. Grimm, F. Hof and A. Hirsch, *J. Mater. Chem. A*, 2013, 1, 11559-11562.

34.   S. Eigler, M. Enzelberger-Heim, S. Grimm, P. Hofmann, W. Kroener, A. Geworski, C. Dotzer, M. Rockert, J. Xiao, C.

Papp, O. Lytken, H. P. Steinruck, P. Muller and A. Hirsch, *Adv. Mater.*, 2013, 25, 3583-3587.

35.   S. Eigler, C. Dotzer, F. Hof, W. Bauer and A. Hirsch, *Chem. Eur. J.*, 2013, 19, 9490-9496.

36.   L. B. Casabianca, M. A. Shaibat, W. W. Cai, S. Park, R. Piner, R. S. Ruoff and Y. Ishii, *J. Am. Chem. Soc.*, 2010, 132, 5672-5676.

37.   A. Lerf, H. He, M. Forster and J. Klinowski, *J. Phys. Chem. B*, 1998, 102, 4477-4482.

38.   A. Lerf, H. Heb, T. Riedl, M. Forster and J. Klinowski, *Solid State Ionics*, 1997, 101-103, 857-862.

39.   W. Cai, R. D. Piner, F. J. Stadermann, S. Park, M. A. Shaibat, Y. Ishii, D. Yang, A. Velamakanni, S. J. An, M. Stoller, J. An, D. Chen and R. S. Ruoff, *Science*, 2008, 321, 1815-1817.

40.   S. Eigler, S. Grimm and A. Hirsch, *Chem. Eur. J.*, 2014, 20, 984-989.

41.   S. Eigler, S. Grimm, M. Enzelberger-Heim, P. Muller and A. Hirsch, *Chem. Commun.*, 2013, 49, 7391-7393.

42.   J. Schneider, M. Matsuoka, M. Takeuchi, J. Zhang, Y. Horiuchi, M. Anpo and D. W. Bahnemann, *Chem. Rev.*, 2014, 114, 9919-9986.

43.   K. D. Asmus, H. Mockel and A. Henglein, *J. Phys. Chem.*, 1973, 77, 1218-1221.

44.   G. V. Buxton, C. L. Greenstock, W. P. Helman and A. B. Ross, *J. Phys. Chem. Ref. Data*, 1988, 17, 513-886.

45.   P. Neta, J. Grodkowski and A. B. Ross, *J. Phys. Chem. Ref. Data*, 1996, 25, 709-1050.

46.   Y. Haas, *Photochem. & Photobiol. Sci.*, 2004, 3, 6-16.

47.   A. Bakac, J. H. Espenson and V. G. Young, *Inorg. Chem.*, 1992, 31, 4959-4964.

48.   M. N. Schuchmann and C. Von Sonntag, *J. Am. Chem. Soc.*, 1988, 110, 5698-5701.

49.   S. Eigler and A. Hirsch, *Angew. Chem. Int. Ed.*, 2014, 53, 7720-7738.

50.   S. Eigler, *Phys. Chem. Chem. Phys.*, 2014, 16, 19832-19835.

51.   A. Kaniyoor and S. Ramaprabhu, *Aip Advances*, 2012, 2.

52.   M. M. Lucchese, F. Stavale, E. H. M. Ferreira, C. Vilani, M. V. O. Moutinho, R. B. Capaz, C. A. Achete and A. Jorio, *Carbon*, 2010, 48, 1592-1597.

53.   L. G. Cançado, A. Jorio, E. H. M. Ferreira, F. Stavale, C. A. Achete, R. B. Capaz, M. V. O. Moutinho, A. Lombardo, T. S. Kulmala and A. C. Ferrari, *Nano Lett.*, 2011, 11, 3190-3196.

54.   S. Eigler, F. Hof, M. Enzelberger-Heim, S. Grimm, P. Müller and A. Hirsch, *J. Phys. Chem. C*, 2014, 118, 7698-7704.

55.   S. Eigler, F. Hof, M. Enzelberger-Heim, S. Grimm, P. Müller and A. Hirsch, *J.Phys.Chem. C*, 2014, 118, 7698-7704.

56.   S. Eigler, *Phys. Chem. Chem. Phys.*, 2014, 16, 19832-19835.

57.   O. Jankovsky, P. Simek, K. Klimova, D. Sedmidubsky, S. Matejkova, M. Pumera and Z. Sofer, *Nanoscale*, 2014, 6, 6065-6074.

58.   L. Huang, Y. Liu, L.-C. Ji, Y.-Q. Xie, T. Wang and W.-Z. Shi, *Carbon*, 2011, 49, 2431-2436.

Nanoscale Accepted Manuscript